# Concept and Prototype Development of Adaptive Touch Walking Support Robot for Maximizing Human Physical Potential

Junya Terayama[1], Ankit A. Ravankar[1], Jose Victorio Salazar Luces[1], Seyed Amir Tafrishi[2] and Yasuhisa Hirata[1]

***Abstract*—We propose a new walking support robot concept, "Nimbus Guardian," designed to enhance the mobility of both healthy and frail elderly individuals who can walk independently. The proposed robot differs from traditional walker-type or cane-type aids by offering adaptive, minimal touch support based on the user's walking dynamics. Our goal is to realize versatile touch to the user as a preliminary study for developing the adaptive touch walking support robot. To achieve this, we have established a categorization system for walking support touch, outlining the specific types of assistance required for our robot. Based on these categorization, we have developed a prototype that improves the versatility of touch support (touch point, force, and initiator), adapting to the user's body. Our prototype is equipped to offer multiple touch support parts, adjusting to the user's physique. For versatile touch capabilities, we designed a motion control algorithm that includes a controller which directs the robot's wheel movements according to the chosen support points, and a state machine that provides multiple arm placements and movements. We have experimentally implemented this motion control algorithm in our prototype. Through experiments, we verified the touch versatility and discussed the prototype's utility and potential for further development.**

***Index Terms*—Human-Centered Robotics, Physically Assistive Devices, Motion Control.**

## I. Introduction

DEMOGRAPHIC shifts due to the aging population and the shortage of caregivers worldwide have led to an increasing demand for the independence of the elderly in their daily lives. To promote independent living, it is important for both healthy and frail elderly individuals to maintain their physical strength and health through daily walking. On the other hand, falls are a major cause of injury and death among the elderly [1], necessitating support to reduce the risk of falling while walking. However, if such support is excessive, the assisted person may not be able to fully utilize their physical potential. Therefore, a walking support robot that reduces the risk of falls and injuries, while maximizing the walker's physical potential by providing minimally necessary and appropriate support according to the situation, is required.

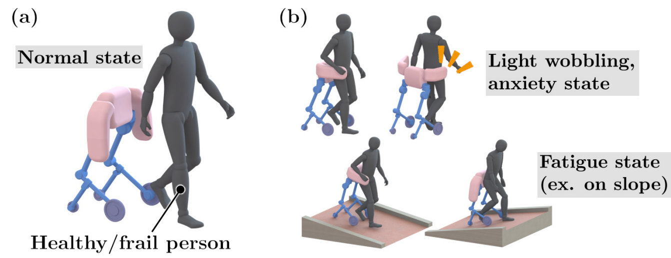


Fig. 1. The concept of a adaptive touch walking support robot, Nimbus Guardian for supporting healthy and frailty person. It provide versatile touch support according to the users' various state.

In this letter, we propose Nimbus Guardian (Nimbus-G), a type of Robotic Nimbus [2], an adaptive touch walking support robot to support healthy and frail elderly, as shown in Fig. 1. The proposed robot is part of a newly initiated project by the Japan Science & Technology called the Moonshot R&D program [3] and aims at solving the superaging problem in Japan by developing advanced support robots for homes and welfare facilities, with a target year of 2030 [4]. The framework involves developing new assistive robots designed to improve welfare and care facilities by using AI-enabled robot technology. These robots, known as 'Robotic Nimbus,' are intended to provide personalized support to elderly individuals, either through a single robot or a coordinated group.

The concept of Nimbus-G is to accompany the user in stable walking without touching (Fig. 1(a)), and to provide various force levels of support such as light touch, motion assist and fall prevention to the necessary point with appropriate initiative (passive or active) according to the user's situation (Fig. 1(b)). The adaptive touch walking support enables the user to maximize the physical potential according to the user's current state when walking. In this letter, as a preliminary study to realize adaptive touch support, we develop a prototype that realizes versatile touch styles (touch point, force, and initiative) to the walking user.

## II. Related Works

The conventional ground walking support robots are primarily classified into lower limb-wearing type [5], [6], walker type [7]–[15] and cane type [16]–[23]. Here, we mainly focus on the cane type and the walker types as mobile robots. In addition, we introduce light touch support and human-robot

Manuscript received: January 22, 2024; Revised April 22, 2024; Accepted June 2, 2024. This paper was recommended for publication by Editor Ryu Jee-Hwan upon evaluation of the Associate Editor and Reviewers' comments. This work was partially supported by JST Moonshot R&D Grant Number JPMJMS2034, JST SPRING Grant Number JPMJSP2114 and JSPS KAKENHI Grant Number JP23KJ0104 & JP21K14115. (Corresponding author: Junya Terayama.)

[1]Junya Terayama, Ankit A. Ravankar, Jose Victorio Salazar Luces and Yasuhisa Hirata are with the Department of Robotics, Tohoku University, Sendai 980-8579, Japan (j.terayama, j.salazar, ankit, hirata@srd.mech.tohoku.ac.jp)

[2]Seyed Amir Tafrishi is with the School of Engineering, Cardiff University, Cardiff, CF24 3AA, Wales, UK (TafrishiSA@cardiff.ac.uk)

Digital Object Identifier (DOI): see top of this page.

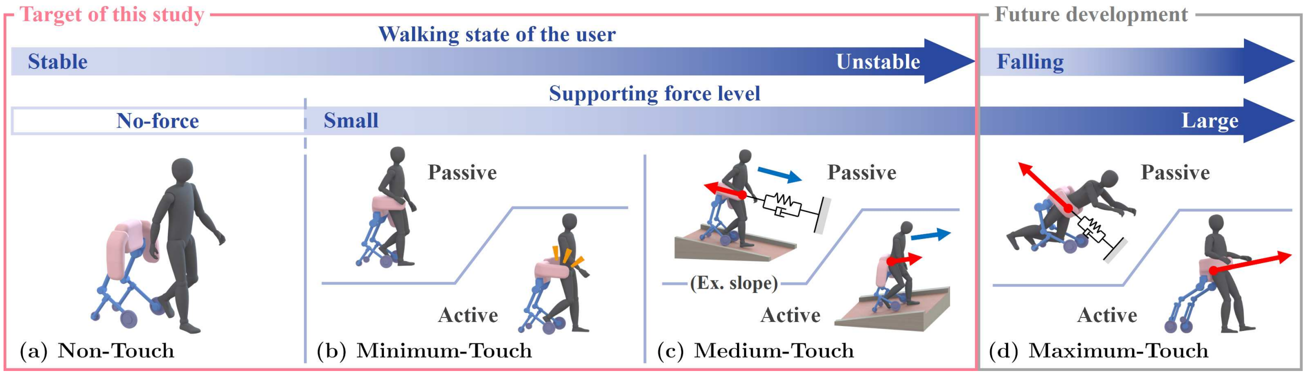


Fig. 2. The touch categories on walking support and the target of this study. The touch support is categorized as minimum, medium, and maximum based on the level of support as active and passive with respect to whether the robot or the user was in the initiative. The target touch that is validated in this study is Non-Touch, Minimum-Touch, and Medium-Touch.

touch interaction, which may extend the scope of adaptive touch walking support, and also describe specific usability of this study.

Walker-type robots provide hand or hip support, tailored for specific disabilities, physical abilities, or environments. Hand support includes an intelligent walkers based on passive robotics [7], a walker with both passive and active control modes [8], an omni-wheel type that supports omni-directional movement [9], and a user-intent-based control system [10] have been proposed in the past. Meanwhile, for waist support, a non-wearing walker that promotes independent pelvic movement [11], a wearing walker that supports pelvic movement together with weight-unloading [12]–[14], and a system that integrates a walking assist robot and an electric wheelchair [15] have been developed.

The cane-type robot supports the user's one hand, and is designed for frail users and users with minor walking disabilities. An omniwheeled cane robot [16] that can assist in all directions on a slope, a fall detection and prevention system [17], a lighter and more compact inverted pendulum type [21], a non-contact tracking control system [18], [23], and a gait analysis system [19] have been developed in the past.

On the other hand, in the field of physical therapy, light touch (less than 1N) from the fingertips has been reported to be effective in maintaining posture [24] and can improve balance even when it is not sufficient to provide physical support to the body [25]. In addition, it has been reported that light touch support to various locations on the back also reduced the swaying [26]. Some previous studies have verified the effectiveness of light touch using a cane-shaped robot [20], [22], but primarily focusing on active user touch.

In the field of human-robot interaction, it has been reported that touch from a robot and its positive actions have an effect on trust [27], hand shakes with robot increases motivation [28], active and passive touch boosts effort [29], and hugging has an effect on happiness and enjoyment [30]. Appropriate touch positively impacts human psychology, with robots accompanying pedestrians receiving higher ratings than walking alone [31].

While conventional robots have distinct characteristics and advantages, they often specialize in specific touch styles, limiting versatility. Exoskeletons and walkers excel in forceful touch, like slope assistance or fall prevention, requiring continuous body contact. For example, many exoskeleton and walker types are good at strong force touch, such as assisting on slopes or preventing falls, but require constant contact between the body and the robot. On the other hand, the intelligent cane [16]–[20] aims for versatility in support, including non-touch accompanying, but the touch point is limited to one hand. Such a specialized approach requires multiple robots to cooperate when adapting to users' different situations and preferences, resulting in problems with the versatility and adaptability of touch style. In addition, there is evidence that light touch and non-contact interactions have positive effects on human walking and psychology [20], [22], [24]–[31], so extending the support to these areas may better encourage walking by leveraging one's physical potential.

The main contribution of this study is the concept of an adaptive touch walking support robot that transcends traditional touch style constraints, and the development of a versatile-touch-style prototype. This novel approach enables multiple touch styles on a single platform, potentially providing more appropriate support to users and revolutionizing their experience.

## III. Touch Categories on Walking Support

### A. Touch force

In order for walking support robots to provide the minimal necessary support for various user states, it is necessary to categorize the versatile touch support in a specific way. Therefore, we categorize four types of touch methods, Non-Touch, Minimum-Touch, Medium-Touch, and Maximum-Touch, based on the user's walking state and the level of contact force, as shown in Fig. 2. The details of each touch are as follows:

- Non-Touch: Support without contact.
- Minimum-Touch: Light touch to alert, motivate, and stabilize walking by the user's own effort in potentially risky situations.
- Medium-Touch: Physical assistance for walking when there's a high risk of instability.
- Maximum-Touch: Support to prevent falls or manage safe falls when independent walking is not possible.

By appropriately selecting these touch methods, the user can challenge themselves to walk to their fullest potential, without

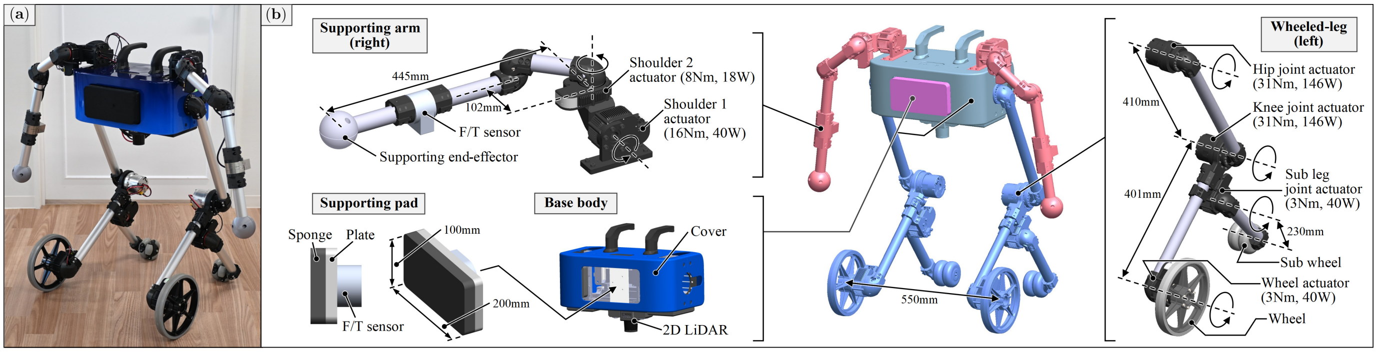


Fig. 3. Developed Nimbus Guardian prototype description. (a) the developed hardware appearance, (b) the configuration of the prototype. The prototype consists of a base body, two-wheeled legs, a dual supporting arm, and a support pad. The actuator of each joint is labeled with its rated torque and output.

being excessively restrained by the robot, while simultaneously minimizing the risk of falls and subsequent injuries.

### B. Touch Initiative

To respect the user's intention in walking, it is preferable for the robot to adopt a passive role in response to contact initiated by the user. Conversely, when there is an increased risk of falling due to solely respecting the user's walking support, the robot should actively initiate contact for support. Therefore, we categorize the robot's touch initiative as follows:

- Passive: A state where the robot remains passive, reacting only to external forces exerted by the human.
- Active: A state where the robot proactively initiates contact with the human, applying external force when needed.

By appropriately selecting the touch initiative from the robot's perspective, appropriate support can be provided to the user according to the situation, and the user's independent walking can be encouraged.

## IV. The Prototype of Nimbus Guardian

### A. Target Walking Support

The prototype of Nimbus Guardian discussed in this letter targets touch support for both healthy and frail elderly individuals during walking. Specifically, we have developed a prototype that enables Non-Touch, Minimum-Touch, and Medium-Touch. The touch-assistive regions are the hands and hips of a person. The effectiveness and versatility of these touch-assistive features using this prototype are presented in Section VI, and their extension to a robot capable of providing Maximum-Touch support is discussed in Section VII-B.

### B. Prototype Design and Development

*1) Overall Design:* Fig. 3(a) shows the prototype's appearance, and Fig. 3(b) its design configuration and main dimensions. The prototype consists of four main components with distinct functions: two-wheeled legs, a dual supporting arm, a base body with a supporting pad, and it weighs approximately 20 kg in total. Four joints in the hips and knees are driven by eRob Actuators from ZeroErr Control, while the other six joints and two drive wheels are powered by HEBI Smart Actuators from HEBI Robotics. Additionally, three force/torque sensors, PFS055YA251U6 by Reptrino, are installed in the contact support area to capture the interaction forces between the human and the robot.

*2) Supporting Arm:* To facilitate stable contact with both hands of a person when needed, or for active, light touch, the robot is equipped with a supporting hand for human contact. A dual supporting arm was designed and each arm features a 2-DOF serial link structure, which is the minimum degree of freedom (DOF) necessary for effective human contact and unobstructed walking. At the end of each arm, a supporting end-effector and a force/torque sensor are installed. Each joint's displacement and velocity are regulated by a high-level controller utilizing a hybrid position/impedance controller [32] and a lower-level PID controller. The inputs of high-level controller are desired displacement and velocity, and the desired/applied torque displacement and angular velocity. These controllers adjust joint displacements and stiffness based on the arm's state, as detailed in Section V-B. While using the end-effector support, the arm exerts up to 36N vertically and 18N laterally.

*3) Wheeled-Leg:* To accommodate various user physiques and navigate over obstacles such as small steps, the robot requires a versatile movement mechanism for contact support. Consequently, wheeled-legs with auxiliary legs were chosen for this purpose. The wheeled-leg incorporates a four-degree-of-freedom serial link structure, consisting of a hip joint, knee joint, driving wheel, and auxiliary leg joint, with the auxiliary wheel being a passive omni-wheel. Differential motion between the left and right drive wheels enables the robot to move straight or turn on a plane. These drive wheels are governed by both an upper impedance controller and a lower PID controller, as described in next Section V-A, ensuring proper interaction forces at the contact points. In a flat environment where the wheels do not slip, the robot can provide a maximum of 60N in the front-back direction to the user before tipping over. In addition, the maximum velocity in the linear direction is 0.8m/s. Moreover, the expansion of the robot's adaptive environment capabilities through its leg design is further discussed in Section VII-C.

*4) Supporting Pad and Base Body:* To effectively provide support, such as pushing on a person's waist (hip), a contact unit with a substantial area and cushioning is required. As a result, a supporting pad, designed for contact with the human waist, was implemented. This pad comprises of a rigid plate, a sponge for cushioning, and a force/torque sensor, all connected to the base body via the different sensors. The base body serves as the central component, connecting other elements like a PC (Jetson nano), communication devices, and

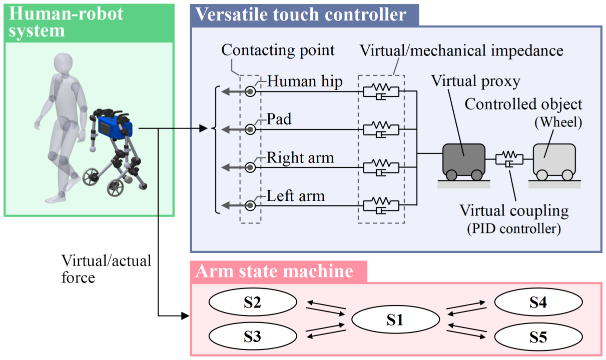


Fig. 4. Overview of the motion control algorithm. This figure illustrates the two main components: the versatile touch controller, which adjusts the robot's movement based on the actual interaction force at the contact point, and the arm state machine, which positions the supporting end-effector and facilitates active touch with the user.

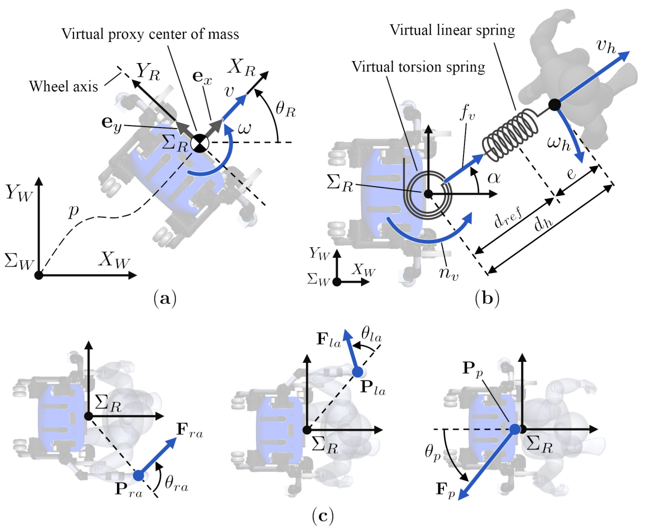


Fig. 5. Human-robot contact model. (a) illustrates the frame and kinematics of the virtual proxy, modeled as a two-wheeled differential robot. (b) depicts the virtual force acting between the robot model and the human in a non-contact scenario. (c) shows the force exerted on the model when the robot is in contact with the user, facilitated by the supporting arm and pad.

a power supply unit, all enclosed by a cover. Additionally, a 2D laser rangefinder, UST-30LX by HOKUYO, is installed at the bottom to localize the person's position, using the centroid of the point cloud for position estimation. The on-board battery (156.3Wh) included in the power supply unit enables continuous operation for approximately two hours.

## V. Motion Control Algorithm

### A. *Versatile Touch Controller*

In order for the robot to offer versatile contact support to a person, it is crucial to control the robot's motion based on the contact point and interaction force between the person and the robot. Hence, a motion control algorithm, including versatile touch control, is proposed, as depicted in Fig. 4. The versatile touch controller determines the target position and velocity to ensure that the virtual proxy in the human-robot contact model, encompassing multiple contact points (the human waist, the pad, the right/left arms), exhibits the desired impedance characteristics. Subsequently, the robot's wheels are operated by a PID controller using these inputs. This subsection primarily focuses on the description of the human-robot contact model within the versatile touch controller.

Firstly, the kinematics of the virtual proxy in the human-robot contact model are outlined. The virtual proxy is modeled as a two-wheel differential robot, with its center of mass located centrally between the driving wheels. The proxy moves with a velocity $v$ in the heading direction ($X_R$) and an angular velocity $\omega$ in the turning direction, and its state variable is represented as $\boldsymbol{\nu} = [v\ \omega]^T$. The equation of motion for the proxy, designed to move with ideal impedance characteristics based on the interaction force between the human and robot, is as follows:

$$\mathbf{M}\dot{\boldsymbol{\nu}} + \mathbf{D}\boldsymbol{\nu} = \mathbf{K}_v\boldsymbol{\tau}_v + \mathbf{K}_{ra}\boldsymbol{\tau}_{ra} + \mathbf{K}_{la}\boldsymbol{\tau}_{la} + \mathbf{K}_p\boldsymbol{\tau}_p \tag{1}$$

where

- $\mathbf{M} \in \mathbb{R}^{2\times 2}$ is the apparent inertia matrix;
- $\mathbf{D} \in \mathbb{R}^{2\times 2}$ is the apparent damping matrix;
- $\mathbf{K}_v\boldsymbol{\tau}_v,\ \mathbf{K}_{ra}\boldsymbol{\tau}_{ra},\ \mathbf{K}_{la}\boldsymbol{\tau}_{la},\ \mathbf{K}_p\boldsymbol{\tau}_p$ are the virtual contact term, the right hand contact term, the left hand contact term, and the hip contact term respectively;
- $\boldsymbol{\tau}_v = [f_v\ n_v]^T \in \mathbb{R}^{2\times 1}$ is the virtual force/moment acting between the person and the robot;
- $\boldsymbol{\tau}_{ra} = \boldsymbol{\tau}_{ra}^H - \boldsymbol{\tau}_{ra}^R, \boldsymbol{\tau}_{la} = \boldsymbol{\tau}_{la}^H - \boldsymbol{\tau}_{la}^R, \boldsymbol{\tau}_p = \boldsymbol{\tau}_p^H - \boldsymbol{\tau}_p^R$;
- $\{\boldsymbol{\tau}_{ra}^H, \boldsymbol{\tau}_{la}^H, \boldsymbol{\tau}_p^H\} \in \mathbb{R}^{2\times 1}$ are the real force/moment from the person to the robot on the right arm, left arm, and the pad respectively;
- $\{\boldsymbol{\tau}_{ra}^R, \boldsymbol{\tau}_{la}^R, \boldsymbol{\tau}_p^R\} \in \mathbb{R}^{2\times 1}$ are the desired actual force/moment from the robot to the human on the right arm, left arm, and the pad respectively;
- $\{\mathbf{K}_v, \mathbf{K}_{ra}, \mathbf{K}_{la}, \mathbf{K}_p\} \in \{\mathbf{0}, \mathbf{I}\}^{2\times 2}$ represents the contact point selection matrix, containing parameters to determine input presence from specific contact points. It can be either a unit matrix $\mathbf{I}$ or a zero matrix. Selecting a unit matrix accepts forces/moments from the corresponding contacting point, while choosing a zero matrix disregards the influence from that contact point.

Next, we describe the inputs to the virtual proxy, which are based on the interaction forces between the person and the robot in each contact term. In the virtual contact term, a virtual interaction force is applied when the proxy is connected to a representative point on the person's waist by a virtual spring. This configuration enables the robot to follow the person without physical contact. The interaction forces are modeled using a virtual linear spring and a virtual torsion spring, as shown in Fig. 5(b). This approach allows for independent control of the linear and rotational responsiveness of the proxy, as:

$$\boldsymbol{\tau}_v = \begin{bmatrix} f_v \\ n_v \end{bmatrix} = \begin{bmatrix} k_f(d_h - d_{ref})\ \cos(\alpha) \\ k_n\alpha \end{bmatrix} \tag{2}$$

where $k_f$ is the spring constant of the linear spring, $k_n$ is the spring constant of the torsion spring, $d_h$ is the distance between the robot and the human, and $d_{ref}$ is the reference length of the linear spring for setting the following distance.

In the right-hand, left-hand, and waist contact terms, the interaction force at each specific contact point—namely, the right and left arm end-effectors and the pads is inputted to ensure that the robot operates based on the actual external

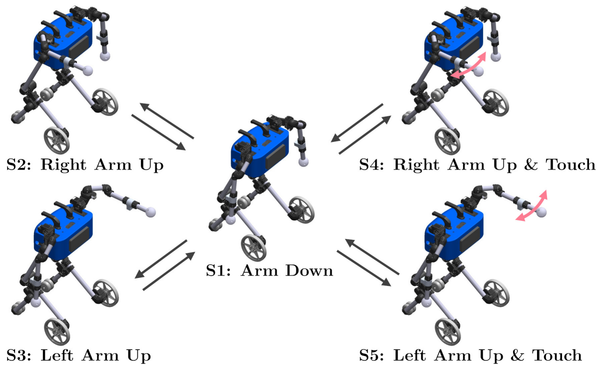


Fig. 6. The five states of the supporting arm controlled by the state machine.

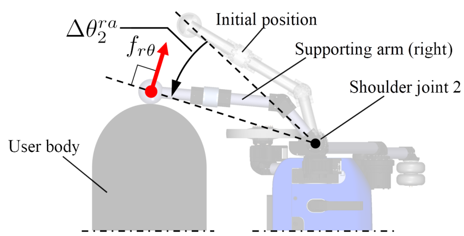


Fig. 7. The top-view schematic of active touch by the right arm. The force from the person is simplified as acting on its end-effector's spherical center.

force exerted by the person. The interaction force applied by the person at each of these contact points is expressed as:

$$\boldsymbol{\tau}_{ra}^{H} = \begin{bmatrix} \mathbf{F}_{ra} \cdot \mathbf{e}_x \\ |\mathbf{F}_{ra}| \cdot |\mathbf{P}_{ra}| \cdot \sin\theta_{ra} \end{bmatrix}, \ \boldsymbol{\tau}_{la}^{H} = \begin{bmatrix} \mathbf{F}_{la} \cdot \mathbf{e}_x \\ |\mathbf{F}_{la}| \cdot |\mathbf{P}_{la}| \cdot \sin\theta_{la} \end{bmatrix},$$
$$\boldsymbol{\tau}_{p}^{H} = \begin{bmatrix} \mathbf{F}_{p} \cdot \mathbf{e}_x \\ |\mathbf{F}_{p}| \cdot |\mathbf{P}_{p}| \cdot \sin\theta_{p} \end{bmatrix} \quad (3)$$

where $\mathbf{e}_x$ is the unit vector in the $X_R$ direction of the robot frame $\Sigma_R$ in the human-robot contact model.

### B. Supporting Arm State Machine

To ensure the contact point in the human-robot contact model supports the human hand effectively, does not interfere with independent walking, and actively touches the human through designed arm joint trajectories, it is necessary to control the trajectory of the supporting arms appropriately according to the situation. The trajectory of the supporting arms is determined by a state machine and controlled in five states (S1-S5), as shown in Fig. 6.

In states S4 and S5, the robot touches the person using shoulder joint 2 of either the right or left arm. The relation between arm joint displacement and force for the right arm is depicted in Fig. 7. Additionally, for touch by the right arm, the process of actively touching the person and returning to the original position at the target time and force involves the following steps:

(a) Set the desired force $f_{r\theta}^{d}$ [N] on the high-level controller, prompting the arm to move toward the person.
(b) When the touch force $f_{r\theta}$ [N] exceeds $\mu$ [%] of the desired force $f_{r\theta}^{d}$, start counting the touch time.
(c) Once the touch time reaches the target time $t_{\mathrm{tch}}$[s], set the target force in the opposite direction and return the arm to its initial position.

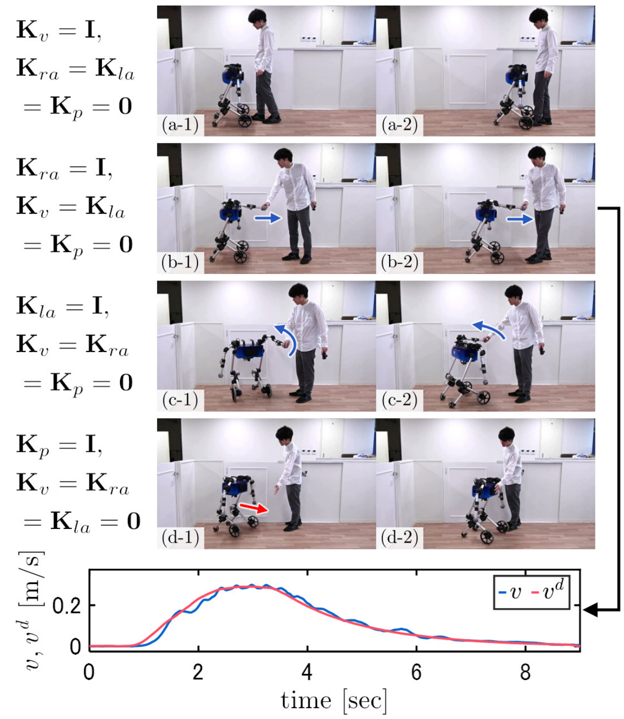


Fig. 8. The experiments of versatile touch controller. By properly selecting the contact term and setting the arm state, the robot can move by either virtual interaction forces or actual interaction forces at the right or left arm, and supporting pad. This demonstrated the ability to support without touching the user and to support the user's right or left hand or hip.

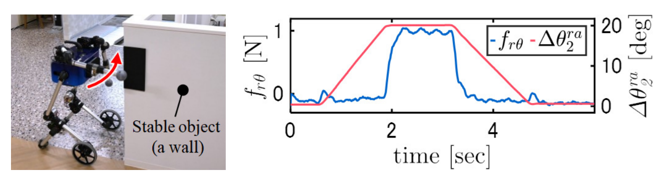


Fig. 9. The experiment of the active touch using the right arm (the state S4). The robot moved its right arm toward a wall, touched the wall with a force of 1N for 1 second, and returned to its original position. This confirmed the ability of the arm to perform active touch.

## VI. EXPERIMENT

### A. Versatile Touch by Motion Control Algorithm

The robot movement experiment utilizing the versatile touch controller is depicted in Fig. 8. It is important to note that the contact terms were pre-set, $\mathbf{I}$ represents the unit matrix, and arm states S1, S2, and S3 were pre-selected based on the contact points. By selecting the contact terms, their values, and the arm states appropriately, various outcomes were verified: non-contact following (Fig. 8(a)), straight and rotational movements initiated by external force on the right and left arms (Fig. 8(b), Fig. 8(c)), and active pushing using pads and stopping due to external force (Fig. 8(d)). It was also observed that the actual velocity effectively tracked the desired velocity $v^d$, calculated based on the external force during linear movement using the right arm (Fig. 8(b)). Readers are recommended to check the accompanying video of the experiments for watching the different levels of touch support.

Additionally, active touch in states S4 and S5 was verified using the right arm. In this experiment, the robot touched

TABLE I
EXPERIMENTAL PARAMETERS OF ADAPTIVE TOUCHING CONTROLLER AND ARM STATE

| Experiment | Touch Initiative | $\mathbf{M}_d$ | $\mathbf{D}_d$ | $\mathbf{K}_v$ | $\mathbf{K}_{ra}$ | $\mathbf{K}_{la}$ | $\mathbf{K}_p$ | $\boldsymbol{\tau}_{ra}^R$ | $\boldsymbol{\tau}_{la}^R$ | $\boldsymbol{\tau}_p^R$ | Arm State |
|---|---|---|---|---|---|---|---|---|---|---|---|
| Non-Touch | —— | diag(15, 2) | diag(10, 5) | $\mathbf{I}$ | $\mathbf{0}$ | $\mathbf{0}$ | $\mathbf{0}$ | $\mathbf{0}$ | $\mathbf{0}$ | $\mathbf{0}$ | S1 |
| Minimum-Touch | Passive | | | | | | | | | | S2 |
| | Active | | | | | | | | | | S4 |
| Medium-Touch | Passive | diag(10, 5) | diag(50, 8) | $\mathbf{0}$ | $\mathbf{0}$ | $\mathbf{I}$ | $\mathbf{0}$ | $\mathbf{0}$ | $\mathbf{0}$ | $\mathbf{0}$ | S3 |
| | Active | diag(15, 2) | diag(10, 5) | $\mathbf{0}$ | $\mathbf{0}$ | $\mathbf{0}$ | $\mathbf{I}$ | $\mathbf{0}$ | $\mathbf{0}$ | $[10, 0]^T$ | S1 |

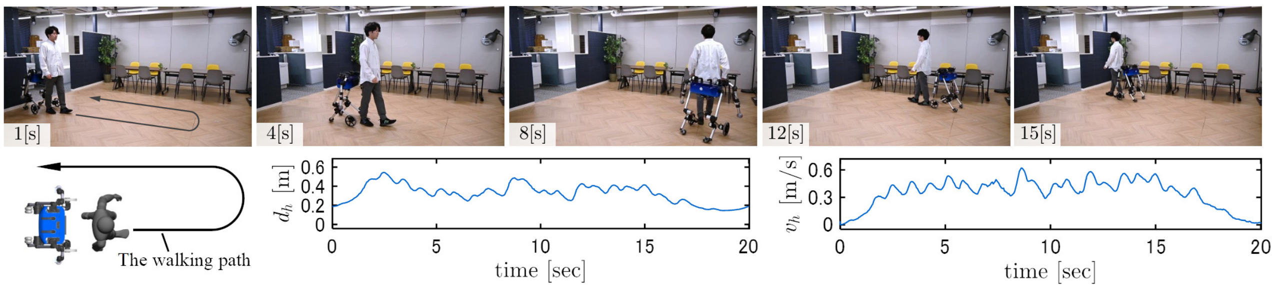


Fig. 10. The experiment of Non-Touch support.

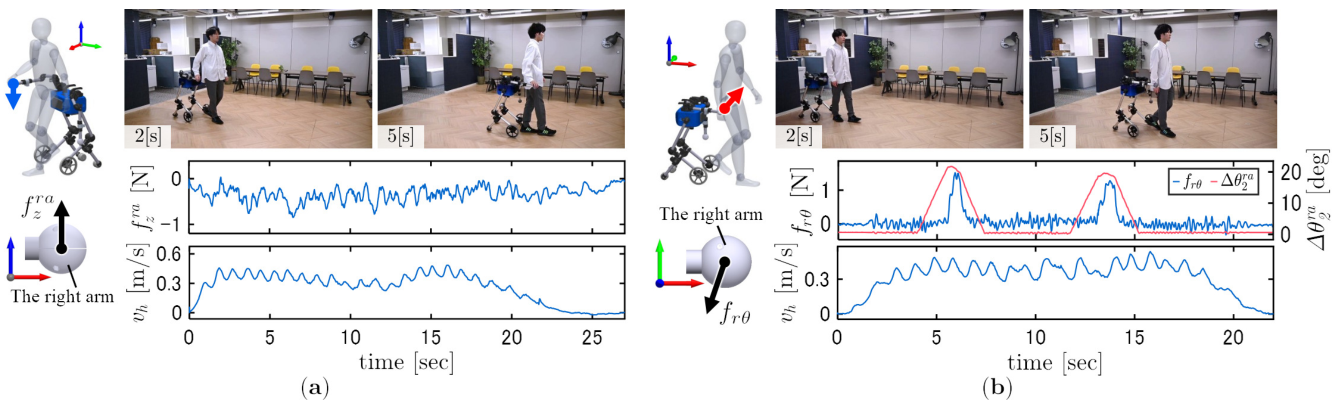


Fig. 11. The experiment of Minimum-Touch support. (a) passive touch initiation and (b) active touch initiation.

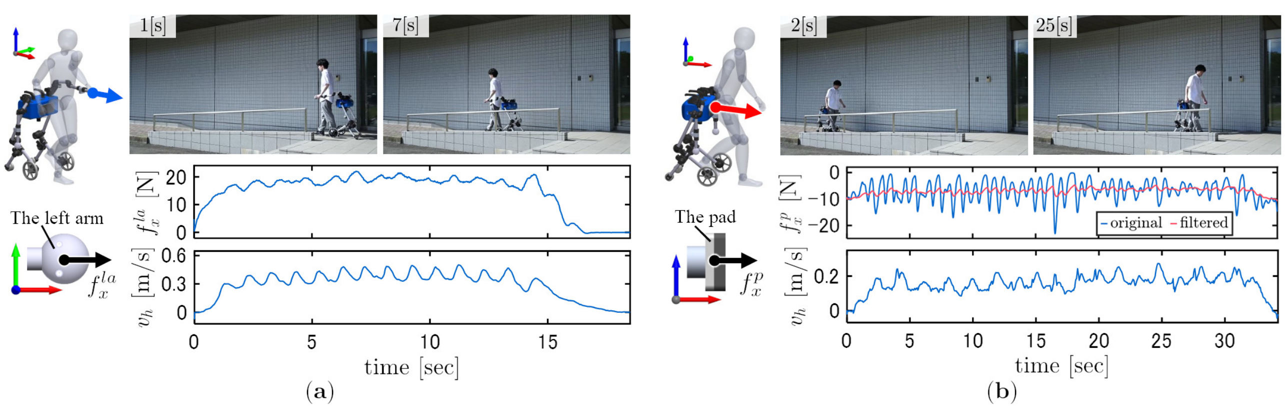


Fig. 12. The experiment of Medium-Touch support. (a) passive touch initiation and (b) active touch initiation.

a stable object (a wall) with parameters $f_{r\theta}^d = 1.0$, $t_{\text{tch}} = 1.0, \mu = 90$. The results, presented in Fig. 9, demonstrate that the robot successfully touched the wall with a force of 1N for 1 second.

These findings confirm the robot's capabilities in non-contact following and both passive and active touching at multiple points. Thus, the robot can achieve versatile contact with a person by appropriately configuring the parameters of the versatile touch controller and the arm state.

### B. Versatile Touch to Walking User

To verify the robot's capability in providing various types of walking support, experiments were conducted to test Non-Touch, Minimum-Touch, and Medium-Touch Support. The target touch force for each assistance is 0N for Non-Touch, less than 3N for Minimum-Touch, and more than 3N for Medium-Touch, and it is checked whether touch at each different force level is achieved for the walking user. It is important to note that the boundary between the target force levels for Minimum-Touch and Medium-Touch is ambiguous, and the target touch force depends on the purpose of the support. For quantitative evaluation, we used a boundary value (3N) based on the maximum touch force employed in a similar human-robot interaction scenario [33]. This defined the highest force considered for measurement and analysis in our experiments. However, further experiments should determine the appropriate touch force ranges according to the touch force categories defined in Section III-A.

Table I lists the versatile touch controller parameters and arm states set for each type of touch support verification. The values for the inertia and damping matrices in the human-robot contact model were determined experimentally. Also, the robot's arm state was preset according to the scenarios.

Moreover, the robot's base body height was adjusted to match the user's lower hip height, and the user's position relative to the robot was estimated using a laser rangefinder at thigh height, to minimize the influence of arm swings.

Fig. 10 illustrates a Non-Touch walking support experiment. Here, a person walks along a U-shaped path composed of straight and curved segments, with the robot following. The virtual contact term parameters, set experimentally, were $k_f = 30, k_n = 10$, with a target distance of $d_{ref} = 0.2$m. The experiment demonstrated that the person completed the path in about 30 seconds, with the robot following at a maximum error of 0.3m, thus confirming Non-Touch support capability at non-contact (touch force 0N).

Fig. 11 details Minimum-Touch support experiments. These tests involved passive (Fig. 11(a)) and active (Fig. 11(b)) light touch assistance while the person traversed a similar U-shaped path. In the passive scenario, the person lightly rested their hand on the robot's arm end-effector. In the active scenario, the robot initiated light touch as $f^d_{r\theta} = 1.0, t_{\mathrm{tch}} = 0.5, \mu = 90$, with the touch timing based on the robot's travel distance. Results showed that in the passive case, the robot enabled continuous light touch (under 1.0N), while in the active case, it executed two light touches (under 2.0N). Therefore, the robot successfully provided Minimum-Touch support of less than 3N.

Fig. 12 presents Medium-Touch support experiments. These involved passive (Fig. 12(a)) and active (Fig. 12(b)) motion assistance on a $4.0°$ incline. In the passive scenario, the robot provided resistance during downhill walking, preventing excessive acceleration. In the active scenario, it assisted in uphill walking. The results indicated that in the passive case, the robot provided an average resistance force of 18N within 3-13 seconds, and in the active case, it offered an average assist force of 10N when stationary, and 7.0N over 5-30 seconds. Thus, the robot's ability to provide Medium-Touch support at more than 3N was confirmed.

## VII. Discussion

### A. Discussion of Experimental Results and Limitation

In our preliminary research for adaptive touch walking support, we developed a prototype of Nimbus-G to provide versatile touch support for walking users. The experimental evaluation demonstrated the prototype's capability to offer Non-Touch, Minimum-Touch (both passive and active), and Medium-Touch (both passive and active) support, confirming its versatility in terms of touch points, force levels, and initiatives.

While the results of this study are promising, they also highlight areas for further development. The prototype's maximum straight-line speed is 0.8 m/s and it is currently suitable for assisting the elderly who walk slowly, while the average walking speed of a healthy person is 1.17 m/s [34]. For users who desire healthier and faster mobility, appropriate actuators should be selected according to the user's physical potential.

On the other hand, although we have successfully assisted pedestrians in the active touch mode, there is no discussion on the support quality yet. The design of the supporting pad, designed as a simple plate and sponge combination, has particular room for improvement, and the shape, compliance, and other aspects of the design need to be improved to achieve a smoother pressing feel with smaller fluctuations.

In addition, the proposed motion control algorithm does not consider cases in which the robot slips or falls over, so it is limited to use on ground with high friction or at less than maximum supply force. For more practical support, slip detection and consideration of the robot's posture are needed.

### B. Extension to Maximum-Touch Supporting Realization

This letter introduced the Nimbus-G concept, featuring versatile touch support, along with a prototype and motion control algorithm designed for touch supports excluding Maximum-Touch, which focuses on fall prevention and impact reduction. To incorporate Maximum-Touch, Nimbus-G must be capable of withstanding large forces, such as the user's weight and impact force. The current design's small contact support area concentrates load on specific body parts, leading to excessive load or potential slippage. Conversely, traditional walking support robots use a harness for broader support, but this restricts user movement.

Potential solutions include enhancing the supporting arm's degrees of freedom (DOF) to enable the robot to embrace the user [30], and using rigid tip extension structures with skeletal frames to extend the arm into variable wearing arms [35]. Additionally, versatile touch control could be expanded into three dimensions by appropriately adjusting the joint stiffness of the wheeled-leg, a concept not explored in this letter, to facilitate gentle falls that minimize impact.

### C. Extension of adaptive environment using wheeled-legs

Unlike conventional walking support robots that lack legs and have a fixed wheel arrangement, Nimbus-G uses wheeled-legs for mobility, offering greater adaptability, especially in terrains with steps and uneven surfaces. Considering that falls can result from external factors such as challenging step environments, in addition to internal factors like muscle weakness, there's a significant need to evolve conventional walking support robots. These advancements should enable safe support on varied terrains, including steps [36].

Our future objectives include developing a motion control algorithm for the wheeled-legs that can navigate steps during support, using the prototype. Furthermore, we aim to create new prototypes capable of providing touch support for stair walking through the cooperation of multiple robots. This development will be guided by the principles outlined in the CARE framework [4].

## VIII. Conclusion

In this study, we introduced Nimbus Guardian, a walking support robot designed to provide versatile touch support, encouraging both healthy and frail elderly individuals to engage in walking. A prototype and a motion control algorithm were developed, facilitating non-contact following, light touch, and motion assistance at the user's hands and waist. The experimental results affirmed the robot's touch support versatility in terms of force magnitude, initiative, and position. The key contributions of this research include:

- The proposal of Nimbus Guardian, an adaptive touch walking support robot for the elderly.
- The introduction of touch categories for walking support.
- The development of a Nimbus Guardian prototype.
- The creation of a motion control algorithm for versatile touch support.
- The evaluation of touch support versatility by the developed prototype.

The next iteration for future research will focus on enhancing the prototype for more practical walking support. This includes developing touch support components and joint control mechanisms for fall prevention and impact reduction, as well as advancing motion control for better adaptation to environments with steps and stairs.

## References


[1] P. Kannus, H. Sievänen, M. Palvanen, T. Järvinen, and J. Parkkari, "Prevention of falls and consequent injuries in elderly people," The Lancet, vol. 366, no. 9500, pp. 1885–1893, 2005.

[2] K. Okabe and Y. Hirata, "A Study of Management to Develop Adaptable AI-enabled Robots toward Inclusive Society," 2022 61st Annual Conference of the Society of Instrument and Control Engineers (SICE), Kumamoto, Japan, 2022, pp. 1369-1374.

[3] "JST Moonshot R&D Program, Goal 3," https://www.jst.go.jp/moonshot /en/program/goal3/index.html, Accessed on April 15th, 2024.

[4] A. A. Ravankar, S. A. Tafrishi, J. V. S. Luces, F. Seto, and Y. Hirata, "CARE: Cooperation of AI robot enablers to create a vibrant society," IEEE Robot. Autom. Mag., vol. 30, no. 1, pp. 2–16, Mar. 2023.

[5] A. Plaza, M. Hernandez, G. Puyuelo, E. Garces and E. Garcia, "Lower-Limb Medical and Rehabilitation Exoskeletons: A Review of the Current Designs," in IEEE Reviews in Biomedical Engineering, vol. 16, pp. 278-291, 2023.

[6] W. -Z. Li, G. -Z. Cao and A. -B. Zhu, "Review on Control Strategies for Lower Limb Rehabilitation Exoskeletons," in IEEE Access, vol. 9, pp. 123040-123060, 2021.

[7] Y. Hirata, A. Hara and K. Kosuge, "Motion Control of Passive Intelligent Walker Using Servo Brakes," IEEE Trans. Robot., vol. 23, no. 5, pp. 981-990, Oct. 2007.

[8] C. -H. Ko, K. -Y. Young, Y. -C. Huang and S. K. Agrawal, "Active and Passive Control of Walk-Assist Robot for Outdoor Guidance," in IEEE/ASME Trans. Mech., vol. 18, no. 3, pp. 1211-1220, June 2013.

[9] Lee, G., Ohnuma, T. & Chong, N.Y. Design and control of JAIST active robotic walker. Intel. Serv, Robot. 3, 125–135 (2010).

[10] Y. -H. Hsieh, K. -Y. Young and C. -H. Ko, "Effective Maneuver for Passive Robot Walking Helper Based on User Intention," IEEE Trans. Ind. Electron., vol. 62, no. 10, pp. 6404-6416, Oct. 2015.

[11] Ohnuma, T., Lee, G. & Chong, N.Y. Development of JARoW-II active robotic walker reflecting pelvic movements while walking. Intel Serv Robotics 10, 95–107 (2017).

[12] K. -R. Mun, Z. Guo and H. Yu, "Development and evaluation of a novel overground robotic walker for pelvic motion support," 2015 IEEE Int. Conf. Rehabil. Robot., Singapore, 2015, pp. 95-100.

[13] M. Peshkin et al., "KineAssist: a robotic overground gait and balance training device," 9th Int. Conf. Rehabil. Robot., Chicago, IL, 2005, pp. 241-246.

[14] H. Munawar, M. Yalcin and V. Patoglu, "Redundant kinematics and workspace centering control of AssistOn-Gait overground gait and balance trainer," 2016 IEEE Int. Conf. Robot. Automat., Stockholm, Sweden, 2016, pp. 3704-3710.

[15] Li, L., Foo, M.J., Chen, J. et al. Mobile Robotic Balance Assistant (MRBA): a gait assistive and fall intervention robot for daily living. J NeuroEngineering Rehabil 20, 29 (2023).

[16] K. Wakita, J. Huang, P. Di, K. Sekiyama and T. Fukuda, "Human-Walking-Intention-Based Motion Control of an Omnidirectional-Type Cane Robot," in IEEE/ASME Trans. Mech., vol. 18, no. 1, pp. 285-296, Feb. 2013.

[17] P. Di et al., "Fall Detection and Prevention Control Using Walking-Aid Cane Robot," in IEEE/ASME Trans. Mech., vol. 21, no. 2, pp. 625-637, April 2016.

[18] Q. Yan, J. Huang, Z. Yang, Y. Hasegawa and T. Fukuda, "Human-Following Control of Cane-Type Walking-Aid Robot Within Fixed Relative Posture," in IEEE/ASME Trans. Mech., vol. 27, no. 1, pp. 537-548, Feb. 2022.

[19] Q. Yan et al., "Intelligent Gait Analysis and Evaluation System Based on Cane Robot," in IEEE Trans on Neural Sys. Rehabil. Eng., vol. 30, pp. 2916-2926, 2022.

[20] Itadera, S., Aoyama, T., Hasegawa, Y. et al. A clinical pilot study on posture stabilization via light contact with cane-type companion robot. Robomech J 6, 17 (2019).

[21] P. Van Lam and Y. Fujimoto, "A Robotic Cane for Balance Maintenance Assistance," in IEEE Trans on Ind. Informat., vol. 15, no. 7, pp. 3998-4009, July 2019.

[22] D. M. Stramel, R. M. Carrera, S. A. Rahok, J. Stein and S. K. Agrawal, "Effects of a Person-Following Light-Touch Device During Overground Walking With Visual Perturbations in a Virtual Reality Environment," IEEE Robot. Automat. Lett., vol. 4, no. 4, pp. 4139-4146, Oct. 2019.

[23] H. Liu et al., "Close-Range Human Following Control on a Cane-Type Robot With Multi-Camera Fusion," IEEE Robot. Automat. Lett., vol. 8, no. 10, pp. 6443-6450, Oct. 2023.

[24] J.J. Jeka, "Light Touch Contact as a Balance Aid", Physical Therapy, vol. 77, no. 5, pp. 476-487, 1997.

[25] Miyoko Watanabe, Hiroaki Tani, Effects of active and passive light-touch support on postural stability during tandem standing, Journal of Physical Therapy Science, 2020, vol. 32, no. 1, pp. 55-58, 2020.

[26] L. Johannsen, A. Guzman-Garcia and A.M. Wing, "Interpersonal light touch assists balance in the elderly", J. Mot. Behav, vol. 41, no. 5, pp. 397-9, Oct. 2009.

[27] H. Cramer, N. Kemper, A. Amin and V. Evers, "The effects of robot touch and proactive behaviour on perceptions of human-robot interactions," 2009 4th ACM/IEEE Int. Conf. Human-Robot Interact., La Jolla, CA, USA, 2009, pp. 275-276.

[28] J. Avelino et al., "The Power of a Hand-shake in Human-Robot Interactions," 2018 IEEE/RSJ Int. Conf. Intel. Robot. Sys., Madrid, Spain, 2018, pp. 1864-1869.

[29] Shiomi, M., Nakagawa, K., Shinozawa, K. et al. Does A Robot's Touch Encourage Human Effort?. Int. J. Soc. Robot. 9, 5–15 (2017).

[30] Block, A.E., Kuchenbecker, K.J. Softness, Warmth, and Responsiveness Improve Robot Hugs. Int. J. of Soc. Robot. 11, 49–64 (2019).

[31] Deneth Karunarathne, Yoichi Morales, Tatsuya Nomura, Takayuki Kanda, Hiroshi Ishiguro, Will Older Adults Accept a Humanoid Robot as a Walking Partner?, Int. J. Soc. Robot., vol.11, issue 2, pp.343-358, Apr. 2019.

[32] A. Seino, J. Terayama, F. Tokuda, A. Kobayashi and K. Kosuge, "Robot End-effector for Fabric Folding," 2023 IEEE/ASME International Conference on Advanced Intelligent Mechatronics (AIM), Seattle, WA, USA, 2023, pp. 150-155.

[33] T.L. Chen, C.H.A. King, A.L. Thomaz and C.C. Kemp, "An Investigation of Responses to Robot-Initiated Touch in a Nursing Context," International Journal of Social Robotics, vol. 6, no. 1, pp. 141-161, 2014.

[34] Cesari, M. et al., "Prognostic value of usual gait speed in well-functioning older people—results from the Health, Aging and Body Composition Study," Journal of the American Geriatrics Society, vol. 53, no. 10, pp. 1675-1680, 2005.

[35] T. Takahashi et al., "Inflated Bendable Eversion Cantilever Mechanism With Inner Skeleton for Increased Stiffness," IEEE Robot. Automat. Lett., vol. 8, no. 1, pp. 168-175, Jan. 2023.

[36] Stewart-Height, A., Koditschek, D. E., & Johnson, M. J. (2023). Reimagining robotic walkers for real-world outdoor play environments with insights from legged robots: a scoping review. Disability and rehabilitation. Assistive technology, 18(6), 798–818.